Relevance of the complete Coulomb interaction matrix for the Kondo problem: Co impurities in Cu hosts

E. Gorelov,[1] T. O. Wehling,[2] A. N. Rubtsov,[3] M. I. Katsnelson,[4] and A. I. Lichtenstein[2]
[1]*Institut für Festkörperforschung and Institute for Advanced Simulation, Forschungszentrum Jülich, 52425 Jülich, Germany*
[2]*I. Institute of Theoretical Physics, University of Hamburg, 20355 Hamburg, Germany*
[3]*Department of Physics, Moscow State University, 119992 Moscow, Russia*
[4]*Institute for Molecules and Materials, Radboud University of Nijmegen, 6525 ED Nijmegen, The Netherlands*
(Received 11 June 2009; revised manuscript received 5 October 2009; published 26 October 2009)

The electronic structure of a prototype Kondo system, a cobalt impurity in a copper host is calculated, accurately taking into account correlation effects on the Co atom. Using the recently developed continuous-time Quantum Monte Carlo technique, it is possible to describe the Kondo resonance with a complete four-index Coulomb interaction matrix. We demonstrate that a standard practice of using a truncated Hubbard Hamiltonian to consider the Kondo physics can be inadequate. Using the full Coulomb vertex on Co, we study the qualitative dependence of the Kondo resonance on the local coordination.

DOI: 10.1103/PhysRevB.80.155132 PACS number(s): 71.27.+a, 73.20.At, 75.20.Hr

I. INTRODUCTION

Scanning tunneling microscopy has become one of the most basic tools for the manipulation of matter at the atomic scale. Although this experimental technique has reached maturity, the detailed theoretical understanding of experimental data is still incomplete and/or contradictory. One of the most famous examples of atomic manipulation is associated with the Kondo effect[1] observed when transition-metal ions (such as Co) are placed on a metallic surface [such as Cu (111)].[2,3] This Kondo effect is the basis for the observation of surprising phenomena such as quantum mirages[4] and has attracted a lot of attention and interest in the last few years. Early interpretations of these observations were based on the assumption that only surface states of Cu (111) are involved in the scattering of electron waves by the Co adatoms.[5–7] However, later experiments with Co atoms on the Cu (100) surface (that does not have any surface state)[8] or in Cu (111) but close to atomic surface steps (that affect the surface states)[9] have indicated that bulk rather than surface states are responsible for the Kondo effect in these situations. The latter can be important for fine tuning of surface electronic structure, with potential applications to nanotechnology. A recent study of $CoCu_n$ clusters on Cu (111) demonstrated this tunability by atomic manipulation and showed that each atom in the vicinity of the magnetic impurity matters for determining the Kondo effect.[10] Moreover, the relevance of the Kondo effect for the electronic structure of metal surfaces themselves was demonstrated by the discovery of a sharp density-of-states peak on the Cr (001) surface and its possible interpretation as an orbital Kondo resonance.[11–13]

At the same time, when calculating the Kondo temperatures for real electronic structures a mapping onto one-orbital Anderson impurity model[14] was used. The realistic atomic geometry of Kondo systems plays a crucial role in complex electronic properties[10,15] and it is, *a priori*, not obvious that a one-orbital Anderson impurity approach is sufficient; even the two-orbital Anderson model demonstrates Kondo physics essentially different from the single-orbital one.[16] A recent theoretical investigation of Fe impurities in gold and silver showed that the proper Kondo model corresponds to a $S=3/2$ spin state.[17] A realistic, multiband consideration of correlation effects in specific solids is possible in the framework of the local-density approximation+dynamical mean-field theory (LDA+DMFT) approach (for review, see Ref. 18). However, formally accurate Quantum Monte Carlo (QMC) calculations[19] are always done with taking into account only the diagonal part of Coulomb interaction,[20,21] even with realistic hybridization functions obtained in the LDA. This approximation is, strictly speaking, uncontrollable. At the same time, approximate schemes working with the complete Coulomb interaction matrix such as the perturbative scheme[22] which is frequently used to calculate electronic structure of transition metals and alloys[23–26] are not sufficient to reproduce so subtle correlation features as the Kondo effect, properly. As for the exact diagonalization[11,12] or numerical renormalization-group[12,16,27] methods they are hardly applicable, due to computational problems, for more than two orbitals per impurity.

The recent progress in continuous-time QMC scheme (CT-QMC) (Refs. 28 and 29) makes it possible to treat the complicated Kondo systems.[30] Here we will apply this method to calculate Kondo temperatures as well as spectral functions for the case of a Co impurity in bulk Cu, in a Cu (111) surface, and on top of a Cu (111) surface. In contrast with all previous calculations we will work with an accurate complete Coulomb interaction U matrix for correlated d orbitals. The latter can be calculated from first principles in a parameter-free way by the GW technique[31] so this approach is completely *ab initio*. Moreover, the CT-QMC method allows to work, without any essential difficulties, even with the rigorous frequency-dependent U matrix. As the first step, we present calculations for the static U matrix but this restriction is purely technical and can be relatively easily removed in the future, with a growth of available computer resources.

II. MULTIORBITAL CT-QMC FORMALISM

The multiorbital impurity problem with a general U matrix is described by the effective action,

$$S_{imp} = S_0 + S_{int} = -\sum_{ij\sigma} \int_0^\beta \int_0^\beta \mathcal{G}_{ij}^{-1}(\tau - \tau') c_{i\sigma}^\dagger c_{j\sigma} d\tau d\tau' + \frac{1}{2} \sum_{ijkl\sigma\sigma'} \int_0^\beta U_{ijkl} c_{i\sigma}^\dagger c_{j\sigma'}^\dagger c_{k\sigma'} c_{l\sigma} d\tau, \quad (1)$$

where i,j,k,l are orbital indices and σ,σ' are spin indices, $\mathcal{G}_{ij}$ is the local noninteracting Green's function for correlated orbitals obtained from the density-functional theory (DFT) with the help of optimal projection operator to the impurity d states,

$$\mathcal{G}_{ij}(i\omega_n) = \sum_{n\mathbf{k}} \frac{\langle d_i|\psi_{n\mathbf{k}}\rangle\langle\psi_{n\mathbf{k}}|d_j\rangle}{i\omega_n + \mu - \varepsilon_{n\mathbf{k}}}, \quad (2)$$

here $\varepsilon_{n\mathbf{k}}$ is the energy spectrum and $\psi_{n\mathbf{k}}$ is the corresponding wave function of our system (metal host with magnetic impurity), described by d_i localized orbitals, and U_{ijkl} is the Coulomb interaction matrix element,

$$U_{ijkl} = \langle i_1 j_2 | V_{12}^{ee} | k_2 l_1 \rangle \quad (3)$$

here $i_1 \equiv d_i(\mathbf{r}_1)$ is local orthogonal wave function for correlated orbitals and V_{12}^{ee} is screened spin-independent Coulomb interaction between electrons at the coordinates $\mathbf{r}_1$ and $\mathbf{r}_2$. We used standard quasiatomic LDA+U parametrization of Coulomb matrix for d electron via effective Slater integrals or average Coulomb parameter U and exchange parameter J as described in Ref. 32. We choose the orbital basis related to spherical harmonics to be sure that the magnetic orbital quantum numbers in the U_{ijkl} matrix satisfy the following sum rule: $i+j=k+l$. In this case we will get rid of so-called three-site terms such as U_{ikkl} with $i \neq l$ which turns out to result in a strong sign problem in QMC calculations with real spherical harmonics.

Following the general CT-QMC scheme[28] we expand the partition function around the Gaussian part of our multiorbital action [Eq. (1)] which gives the fermionic determinant over the noninteracting Green's functions with the rank $2n$,

$$\frac{Z}{Z_0} = \sum_n \frac{(-1)^n}{n!\,2^n} \sum_{\{ijkl\sigma\sigma'\}} \int_0^\beta d\tau_1 \ldots \int_0^\beta d\tau_n U_{i_1 j_1 k_1 l_1} \ldots U_{i_n j_n k_n l_n} \times \det \mathcal{G}^{2n\times 2n}. \quad (4)$$

In order to minimize the number of different interaction vertices we group different matrix elements of the multiorbital Coulomb interactions which have a similar structure of fermionic operators. Since the U_{ijkl} matrix elements are spin independent, one should look over all possible combinations of orbital and spin indices, to generate all terms for the interaction in the action [Eq. (1)]. Some combinations can violate the Pauli principle and should be removed. For CT-QMC algorithm it is useful to represent the interaction Hamiltonian in the following form: $U_{ijkl} c_{i\sigma}^\dagger c_{l\sigma} c_{j\sigma'}^\dagger c_{k\sigma'}$.

The interaction terms can be transformed to the desired form, depending on relations between spin and orbital indices: (i) if $\sigma \neq \sigma'$, we can just commute $c_{l\sigma}$ and $c_{k\sigma'}$ and then $c_{l\sigma}$ and $c_{j\sigma'}^\dagger$. Another combination of indices, that allows the same commutation, is the following: $\sigma=\sigma'$, $i \neq j$, and $k \neq l$ (the latter two are following from the Pauli principle), and also $j \neq l$. These terms we can transform to the following desirable representation:

$$H_{ijkl}^{int\,1} = U_{ijkl} c_{i\sigma}^\dagger c_{l\sigma} c_{j\sigma'}^\dagger c_{k\sigma'}. \quad (5)$$

(ii) In the case when $\sigma=\sigma'$ and $j=l$ we can commute $c_{k\sigma'}$ and $c_{j\sigma'}^\dagger$ since in this case $i \neq j$ and $k \neq l$ due to the Pauli principle,

$$H_{ijkl}^{int\,2} = -U_{ijkl} c_{i\sigma}^\dagger c_{k\sigma} c_{j\sigma}^\dagger c_{l\sigma}. \quad (6)$$

After generating all these terms it is useful to collect and *symmetrize* all the terms with identical and equivalent (i.e., $U_{ijkl} c_{i\sigma}^\dagger c_{j\sigma} c_{k\sigma'}^\dagger c_{l\sigma'}$ and $U_{klij} c_{k\sigma'}^\dagger c_{l\sigma'} c_{i\sigma}^\dagger c_{j\sigma}$) quantum numbers.

In order to reduce the fermionic sign problem we introduce additional parameters, α, to optimize the splitting of the Gaussian and interaction parts of the action [Eq. (1)],

$$S_0 = \sum_{ij\sigma} \int_0^\beta \int_0^\beta \left[-\mathcal{G}_{ij}^{-1}(\tau - \tau') + \frac{1}{2} \sum_{\{kl\sigma'\}} \alpha_{kl}^{\sigma'} (U_{ilkj} + U_{lijk}) \delta_{\tau\tau'} \right] c_{i\sigma}^\dagger c_{j\sigma} d\tau d\tau',$$

$$S_{int} = \frac{1}{2} \sum_{\{ijkl\sigma\sigma'\}} \int_0^\beta U_{ijkl} (c_{i\sigma}^\dagger c_{l\sigma} - \alpha_{il}^{\sigma})(c_{j\sigma'}^\dagger c_{k\sigma'} - \alpha_{jk}^{\sigma'}) d\tau. \quad (7)$$

One can see, that the first item in Eq. (7) on Matsubara frequencies corresponds to bare Green's function,

$$\mathcal{G}_{ij}^{-1} = (i\omega_n + \mu)\delta_{ij} - \Delta_{ij}(\omega_n), \quad (8)$$

where Δ is the hybridization matrix. The second term is just a constant which we can absorb to the new chemical potential $\tilde{\mu}$. Therefore we can rewrite the bare Green's function in the following matrix form:

$$\tilde{\mathcal{G}}^{-1} = (i\omega_n + \tilde{\mu})\mathbf{1} - \mathbf{\Delta}. \quad (9)$$

The optimal choice of parameters α_{ij}^σ would lead to effective reduction in interaction terms in the action [Eq. (7)] and therefore minimization of average perturbation order in Eq. (4).

Note that relation between $\tilde{\mathcal{G}}$ and $\mathcal{G}$ can be represented from Eq. (7) in the following spin and orbital matrix form:

$$\tilde{\mathcal{G}}^{-1} = \mathcal{G}^{-1} - \langle \hat{\alpha}\hat{U} \rangle. \quad (10)$$

Here we used the fact that $U_{ilkj}=U_{lijk}$ following from the definition of the Coulomb matrix elements [Eq. (3)].

We also need to minimize the fermionic sign problem which finally leads us to such expression for diagonal alpha parameters,

$$\alpha_\sigma^{ii} + \alpha_{\sigma'}^{jj} = \bar{\alpha}, \quad (11)$$

corresponding to the following interaction fields: $U_{ijji} n_{i\sigma} n_{j\sigma'}$. The $\bar{\alpha}$ has to be found iteratively in order to get a proper occupation number of correlated electrons. In the case of

half-filled one-band Hubbard model $\bar{\alpha}=1$ leads to the correct chemical-potential shift of the $\frac{U}{2}$ and average $\alpha=\frac{1}{2}$ which corresponds to the Hartree-Fock subtraction. For nondiagonal alpha's which correspond to the fields of general form $U_{ijkl}c^{\dagger}_{i\sigma}c_{l\sigma}c^{\dagger}_{j\sigma'}c_{k\sigma'}$, where $i\neq l$ and $j\neq k$ we find the following optimal condition:

$$\alpha^{ij}_{\sigma}+\alpha^{kl}_{\sigma'}=0. \tag{12}$$

Since we symmetrize the interaction U matrix it is necessary to extend the definition of the $\hat{\alpha}$ matrix to keep all the terms in the interaction part of initial action [the last item in Eq. (7)]. It can be done in the following way:[28,33] for every U_{ijkl} field in 50% of updates we deliver the α parameters as $\alpha^{jl}=\alpha_{diag}$ and $\alpha^{jk}=\bar{\alpha}-\alpha_{diag}$, and in another 50% as $\alpha^{jl}=\bar{\alpha}-\alpha_{diag}$ and $\alpha^{jk}=\alpha_{diag}$ for the case of $i=l$ and $j=k$. For nondiagonal fields, i.e., $i\neq l$ and $j\neq k$ $\alpha^{il}=\alpha_{nd}$, $\alpha^{jk}=-\alpha_{nd}$, with 50% probability and $\alpha^{il}=-\alpha_{nd}$, $\alpha^{jk}=\alpha_{nd}$ otherwise. It was found that the sign problem is eliminated in the case when $\alpha_{diag}<0$ and $\bar{\alpha}\geq 1$ for occupancy $n\geq\frac{1}{2}$ per state and $\alpha_{diag}>0$, $\bar{\alpha}<1$ otherwise. The optimal choice of $|\alpha_{diag}|$ parameter is few percent of $|\bar{\alpha}|$ to keep minimal average perturbation order. Another problem is a proper choice of nondiagonal α_{nd} parameter. It is easy to see that α_{nd} is proportional to acceptance probability of nondiagonal field in the case where corresponding bare Green's function $\mathcal{G}_{jk}=0$. Since these processes are unphysical, the natural choice is $\alpha_{nd}=0$. But it leads to division by zero in the updating the inverse Green's-function matrix.[28] On the other hand increasing the α_{nd} parameter causes a sign problem. We find a reasonable choice of α_{nd} to be on the order of 10^{-4}. Moreover for some special cases such as the atomic limit, where $\mathcal{G}_{mm}(\tau)$ is constant, a small noise should be added to all the α parameters to avoid numerical divergency.

III. RESULTS

The Co-Cu system is treated as five-orbital impurity model representing $3d$ electronic shell of the cobalt atom hybridized with a bath of a conduction Cu electrons. We consider Co impurity atoms in the bulk as well as in and on the Cu (111) surface to study the effect of decreasing the coordination of the magnetic impurity from 12 in the bulk, via 9 in the surface to 3 on top of the surface. In all cases, the bath Green's function was obtained using the first-principles DFT within the supercell approach. The DFT calculations were carried out with the Vienna ab initio simulation package (VASP) (Refs. 34 and 35) using the projector-augmented wave (PAW) basis sets.[36] The simulation of a cobalt impurity in the bulk employed a $CoCu_{63}$ supercell structure with the lattice constant corresponding to pure copper. The surfaces were modeled by supercells of Cu (111) slabs containing five Cu layers with 2×2 and 3×4 lateral extension for Co in and on the surface, respectively. The PAW basis naturally provides the projectors $\langle d_i|\psi_{n\mathbf{k}}\rangle$ required in Eq. (2). In using these PAW projectors, directly, we employ here the same representation of localized orbitals as used within the LDA $+U$ scheme implemented in the VASP code itself or as discussed in the context of LDA+DMFT in Ref. 37.

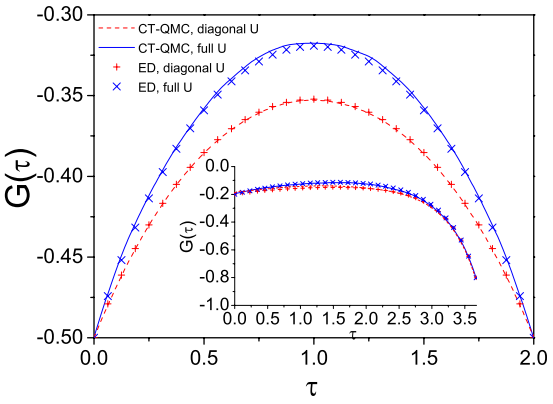

FIG. 1. (Color online) Comparison with ED in the atomic limit (without hybridization to the bath of free electrons). Main graph: $U=1$ eV, $J=0.4$ eV and $\beta=2$ eV^{-1}, for five-orbital impurity at half filling; inset: $U=2$ eV, $J=0.7$ eV, and $\beta=3.7$ eV^{-1}, for five-orbital impurity with eight electrons.

For the problem of a single Co impurity in a bulk copper matrix the basis set of spherical harmonics Y_{lm} is used. In this basis the interaction part of the Hamiltonian contains only terms of the following form: diagonal density density such as $H^{diag}_{int}=U_{iji}n_{i\sigma}n_{j\sigma'}$, where $n_{i\sigma}=c^{\dagger}_{i\sigma}c_{i\sigma}$ and nondiagonal $H^{nd}_{int}=U_{ijkl}c^{\dagger}_{i\sigma}c_{j\sigma'}c^{\dagger}_{k\sigma'}c_{l\sigma}$, where $i\neq j$ and $k\neq l$. The Coulomb matrix for the d-electron shell in the basis of complex harmonics contains 45 nonequivalent diagonal terms. Nondiagonal terms can be further classified into spin flips, where $i=l$ and $j=k$ and the most general four-orbital interactions, where this condition is not fulfilled. Notice, that pair-hopping terms $(i=k,j=l)$ are restricted by symmetry in this basis. In description of d-electron shell we have to involve 20 nonequivalent spin flips and 64 terms of the most general form.

To find the effects, caused by nondiagonal terms, we used two different interaction Hamiltonian. First, interaction with only diagonal terms was used. In this case there is no sign problem. Then, the complete Coulomb interaction matrix of the $3d$-electron shell of the cobalt atom with 129 terms was included.

As a benchmark we use impurity problem in the atomic limit since it can be compared with the result of exact diagonalization (ED) method. The results for the imaginary time Green's function for a five-orbital model with different chemical potentials corresponding to the d^5 and d^8 configurations are shown in the Fig. 1 in comparison with ED results. The significant difference between density-density (diagonal) interaction and the full vertex can be found both at half-filled case with relatively high temperature with the $U=1$ eV, $J=0.4$ eV, and $\beta=2$ eV^{-1} and at nonsymmetric case even for lower temperature. Note that in the d^8 and d^7 cases the many-body ground states have different symmetry for diagonal interactions and nondiagonal full vertex. The results for d^8 configuration with the interaction parameters $U=2$ eV, $J=0.7$ eV, and $\beta=3.7$ eV^{-1} are shown in the inset of the Fig. 1. The difference between Green's function of the interacting system with full Coulomb interaction and density-density one is visible on the $G(\tau)$. We find a very good agreement between CT-QMC results and ED solution.

In the inset of Fig. 2 we show the distribution of nondiagonal terms, i.e., the contribution of Coulomb fields of the

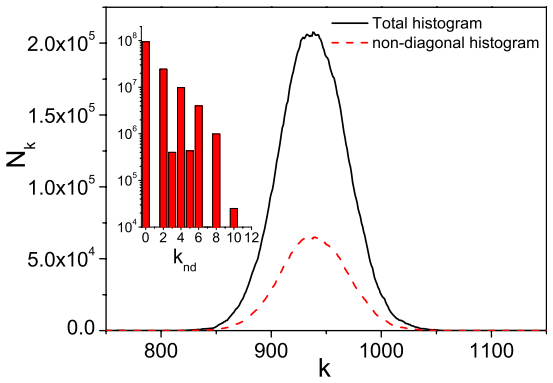

FIG. 2. (Color online) Histograms of Monte Carlo distributions for average perturbation order. Main graph: $U=4$ eV, $J=0.7$ eV, and $\beta=10$ eV^{-1} for five-orbital impurity coupled to realistic Cu bath with seven electrons; inset: $U=4$ eV, $J=0.7$ eV, and $\beta=1$ eV^{-1} in the case of five-orbital impurity model, coupled to semielliptical bath with bandwidth $W=0.5$ eV at the half filling.

form (5) to the resulting Green's function. The zero entry of this histogram counts the number of steps when all the fields contributing to the fermionic determinant [Eq. (4)] were of density-density type. The entry with index 2 show us the number of steps where the average [Eq. (4)] was containing two spin-flip-type fields [Eq. (5)]. Such situation takes place, for example, when one Coulomb field representing spin-flip $c^{\dagger}_{i\uparrow}c_{j\downarrow}c^{\dagger}_{i\downarrow}c_{j\uparrow}$ process was used to construct the determinant.

One can see in the inset of Fig. 2, that only even orders of interaction histogram have large acceptance probability at high temperature and even the tenth order in nondiagonal interactions has nonzero contribution. The third- and fifth-order contributions exist due to the finite α^{nd} parameter.

Typical distribution of the perturbation order (five-orbital AIM with seven electrons, $U=4$ eV, $J=0.7$ eV, and $\beta=10$ eV^{-1}) is shown in Fig. 2, main plot. Dash line denotes the perturbation order during accepted steps that involved nondiagonal fields. The coincidence of distributions maxima of both histograms demonstrate that the acceptance rate mostly depends on diagonal interactions.

For many-body calculations of the Co impurity in the Cu matrix we need to find the effective d-orbital chemical potential which defines the number of $3d$ electrons of cobalt. The particular electronic configuration of a Co atom in a copper matrix is unknown but the DFT results ($n_d=7.3$) give us an evidence that it is close to d^7 configuration. Therefore we performed all impurity calculations for cobalt d^7 configuration. The density of states being discussed in the following have been obtained from the QMC Matsubara Green's functions by analytical continuation using the maximum entropy method.[38]

The results of the CT-QMC calculations for $U=4$ eV and $J=0.7$ eV are presented in Fig. 3 compared to the bare impurity density of states for cobalt impurity in the bulk. There is a pronounced difference between Kondo-type resonance near the Fermi level. In the case of full U vertex it becomes more narrow and located much closer to the Fermi level. The sign problem for realistic five-band model depends crucially on the symmetry of Coulomb Vertex U_{ijkl} and magnitude of nondiagonal terms in the bath Green's functions $\mathcal{G}_{ij}$. The

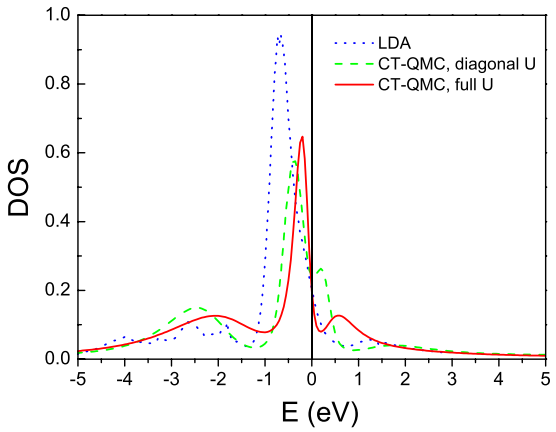

FIG. 3. (Color online) Total DOS of $3d$ orbital of Co atom embedded in Cu matrix. Model parameters: $U=4$ eV, $J=0.7$ eV, and $\beta=10$ eV^{-1} for five-orbital impurity with seven electrons.

most serious problem is related with nondiagonal terms of U matrix, therefore we use a basis of complex spherical harmonics. In this case there is no so-called three-cite terms or correlated hopping, e.g., U_{ikkl}. On the other hand, in this basis, the bath Green's-function matrix $\mathcal{G}_{ij}$ for d electrons has two nondiagonal elements in the bulk of cubic crystals and much more on the surface and in the first layer. Moreover there are a lot of small four-site terms U_{ijkl} which result in a large sign problem for surface adatom calculations. The sign problem for a Co impurity in the bulk is not large and average sign is between 0.90 and 0.97 depends on the simulation temperature.

In the case of nondiagonal interaction we used so-called cluster steps which correspond to complex Monte Carlo updates with more than one additional interaction field. This scheme became essential for spin-flip-type interaction or more general U vertex which can contribute to the Green's function only in the second- or higher-order "diagrammatic" expansion and this can let the Monte Carlo process to explore all the phase space. We note that probability of nondiagonal terms drastically decrease with increasing the hybridization to the bath. Nevertheless, at least for three-band benchmarks we found remarkable effect of the spin-flip terms if the bath Green's function has peaks in the vicinity of the Fermi level on the distance on the order of J.

We estimated the renormalization factor $Z=(1-d\Sigma/dE)^{-1}$ for $U=4.5$ eV, $J=0.7$ eV, and $\beta=10$ eV^{-1} and find $Z_{t_{2g}}=0.5$ and $Z_{e_g}=0.4$ which shows the reasonably strong interaction of Co d electrons. We estimate the Kondo temperature (T_K) using the temperature dependence of full width at half maximum for resonance near Fermi level. Since our simulation temperature is very high compared to T_K we can get only order of magnitude of $T_K=0.1$ eV, which is reasonable for Co impurity systems.[8]

We also performed the CT-QMC calculation of cobalt impurity on the surface of Cu(111) and embedded into the first copper layer. In contrast to the bulk system the surface one has a large sign problem, related with the relatively large nondiagonal elements of the bath Green's functions. Although changing of the sign is a very rare event (less than 0.03% of the accepted steps), we used simple constrained

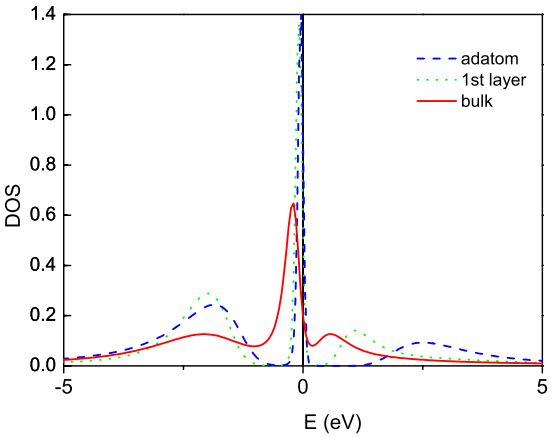

FIG. 4. (Color online)Total DOS of 3*d* orbital of Co atom embedded in the bulk of Cu, into first layer and Co adatom on the Cu(111) surface. Model parameters: $U=4$ eV, $J=0.7$ eV, and $\beta=10$ eV^{-1} for five-orbital impurity with seven electrons.

sign calculations. This sign problem prevents us from calculating at sufficiently low temperatures, which would be required for reliably obtaining a quantitative value of the width of the Kondo resonance. However, a qualitative study of how the local coordination affects the spectral properties of the impurity is possible at $\beta=10$ eV^{-1}. A comparison of the different spectral functions for the bulk-, surface-, and first-layer cobalt impurity is presented in Fig. 4. One can see clearly the change in the Kondo resonance width as a function of reduced dimensionality, i.e., when going from the bulk into or on the surface. At our simulation temperature, the width of the Kondo resonance of Co in and on the surface appears to be similar. However, the high-energy features of the spectra differ markedly between Co on and in the surface. The upper Hubbard peak is shifted to higher energies upon reducing the coordination.

IV. CONCLUSIONS

We performed continuous-time QMC calculation of Co impurities in copper and consider a realistic five-orbital Anderson impurity model including the full Coulomb matrix. The relevance of the nondiagonal part of the Coulomb matrix in the Kondo problem is discussed. Comparing Figs. 3 and 4 we find that nondensity-density terms in the Coulomb vertex are required to obtain quantitative predictions of spectral functions and related properties. The position of the Hubbard peaks and the Kondo peak is markedly changed by spin flips and other nondiagonal terms of the Coulomb vertex. Thus, obtaining sensitive observables such as Kondo temperatures quantitatively requires accounting for these terms. On the other hand hybridization effects such as bringing the Co impurity from bulk to the surface and having it on top of the surface can be quite drastic. As Fig. 4 shows, the sharpening of the Kondo resonance and the shifting of the Hubbard bands is much stronger when going from bulk to the surface than on switching on the nondiagonal part of Coulomb matrix. Only the qualitative overall shape of the DOS and its response to strong hybridization changes are well described by density-density-type terms of the Coulomb vertex.

ACKNOWLEDGMENTS

The authors acknowledge a financial support from DFG SFB-668 (Germany), RFFI (Russia), and FOM (The Netherlands).

[1] A. C. Hewson, *The Kondo Problem to Heavy Fermions* (Cambridge University Press, Cambridge, 1993).
[2] V. Madhavan, W. Chen, T. Jamneala, M. F. Crommie, and N. S. Wingreen, Science **280**, 567 (1998).
[3] J. Li, W.-D. Schneider, R. Berndt, and B. Delley, Phys. Rev. Lett. **80**, 2893 (1998).
[4] H. C. Manoharan, C. P. Lutz, and D. M. Eigler, Nature (London) **403**, 512 (2000).
[5] G. A. Fiete and E. J. Heller, Rev. Mod. Phys. **75**, 933 (2003).
[6] O. Agam and A. Schiller, Phys. Rev. Lett. **86**, 484 (2001).
[7] D. Porras, J. Fernández-Rossier, and C. Tejedor, Phys. Rev. B **63**, 155406 (2001).
[8] N. Knorr, M. A. Schneider, L. Diekhöner, P. Wahl, and K. Kern, Phys. Rev. Lett. **88**, 096804 (2002).
[9] L. Limot and R. Berndt, Appl. Surf. Sci. **237**, 572 (2004).
[10] N. Néel, J. Kröger, R. Berndt, T. O. Wehling, A. I. Lichtenstein, and M. I. Katsnelson, Phys. Rev. Lett. **101**, 266803 (2008).
[11] O. Yu. Kolesnychenko, R. de Kort, M. I. Katsnelson, A. I. Lichtenstein, and H. van Kempen, Nature (London) **415**, 507 (2002).
[12] O. Yu. Kolesnychenko, G. M. M. Heijnen, A. K. Zhuravlev, R. de Kort, M. I. Katsnelson, A. I. Lichtenstein, and H. van Kempen, Phys. Rev. B **72**, 085456 (2005).
[13] T. Hänke, M. Bode, S. Krause, L. Berbil-Bautista, and R. Wiesendanger, Phys. Rev. B **72**, 085453 (2005).
[14] Chiung-Yuan Lin, A. H. Castro Neto, and B. A. Jones, Phys. Rev. Lett. **97**, 156102 (2006).
[15] L. Vitali, R. Ohmann, S. Stepanow, P. Gambardella, K. Tao, R. Huang, V. S. Stepanyuk, P. Bruno, and K. Kern, Phys. Rev. Lett. **101**, 216802 (2008).
[16] A. K. Zhuravlev, V. Yu. Irkhin, M. I. Katsnelson, and A. I. Lichtenstein, Phys. Rev. Lett. **93**, 236403 (2004).
[17] T. A. Costi, L. Bergqvist, A. Weichselbaum, J. von Delft, T. Micklitz, A. Rosch, P. Mavropoulos, P. H. Dederichs, F. Mallet, L. Saminadayar, and C. Bäuerle, Phys. Rev. Lett. **102**, 056802 (2009).
[18] G. Kotliar, S. Y. Savrasov, K. Haule, V. S. Oudovenko, O. Parcollet, and C. A. Marianetti, Rev. Mod. Phys. **78**, 865 (2006).
[19] J. E. Hirsch and R. M. Fye, Phys. Rev. Lett. **56**, 2521 (1986).
[20] M. I. Katsnelson and A. I. Lichtenstein, Phys. Rev. B **61**, 8906 (2000).
[21] A. Liebsch and A. Lichtenstein, Phys. Rev. Lett. **84**, 1591 (2000).
[22] M. I. Katsnelson and A. I. Lichtenstein, Eur. Phys. J. B **30**, 9 (2002).

[23] J. Minár, L. Chioncel, A. Perlov, H. Ebert, M. I. Katsnelson, and A. I. Lichtenstein, Phys. Rev. B **72**, 045125 (2005).
[24] A. Grechnev, I. Di Marco, M. I. Katsnelson, A. I. Lichtenstein, J. Wills, and O. Eriksson, Phys. Rev. B **76**, 035107 (2007).
[25] I. Di Marco, J. Minár, S. Chadov, M. I. Katsnelson, H. Ebert, and A. I. Lichtenstein, Phys. Rev. B **79**, 115111 (2009).
[26] S. Chadov, J. Minár, M. I. Katsnelson, H. Ebert, D. Ködderitzsch, and A. I. Lichtenstein, EPL **82**, 37001 (2008).
[27] R. Bulla, T. Costi, and T. Pruschke, Rev. Mod. Phys. **80**, 395 (2008).
[28] A. N. Rubtsov, V. V. Savkin, and A. I. Lichtenstein, Phys. Rev. B **72**, 035122 (2005).
[29] P. Werner, A. Comanac, L. de' Medici, M. Troyer, and A. J. Millis, Phys. Rev. Lett. **97**, 076405 (2006).
[30] V. V. Savkin, A. N. Rubtsov, M. I. Katsnelson, and A. I. Lichtenstein, Phys. Rev. Lett. **94**, 026402 (2005).
[31] F. Aryasetiawan, M. Imada, A. Georges, G. Kotliar, S. Biermann, and A. I. Lichtenstein, Phys. Rev. B **70**, 195104 (2004).
[32] V. I. Anisimov, F. Aryasetiawan, and A. I. Lichtenstein, J. Phys.: Condens. Matter **9**, 767 (1997).
[33] F. F. Assaad and T. C. Lang, Phys. Rev. B **76**, 035116 (2007).
[34] G. Kresse and J. Hafner, J. Phys.: Condens. Matter **6**, 8245 (1994).
[35] G. Kresse and D. Joubert, Phys. Rev. B **59**, 1758 (1999).
[36] P. E. Blöchl, Phys. Rev. B **50**, 17953 (1994).
[37] B. Amadon, F. Lechermann, A. Georges, F. Jollet, T. O. Wehling, and A. I. Lichtenstein, Phys. Rev. B **77**, 205112 (2008).
[38] M. Jarrell and J. E. Gubernatis, Phys. Rep. **269**, 133 (1996).